



# Fractionation of rhenium isotopes in the Mackenzie River basin during oxidative weathering

Mathieu Dellinger<sup>a,\*</sup>, Robert G. Hilton<sup>a</sup>, Geoff M. Nowell<sup>b</sup>

<sup>a</sup> Geography Department, Durham University, South Road, Durham DH1 3LE, UK

<sup>b</sup> Earth Science Department, Durham University, South Road, Durham DH1 3LE, UK



## ARTICLE INFO

### Article history:

Received 15 January 2021

Received in revised form 9 July 2021

Accepted 22 July 2021

Available online 1 September 2021

Editor: L. Derry

### Keywords:

rhenium isotopes  
Mackenzie River  
oxidative weathering  
organic matter

## ABSTRACT

Rhenium (Re) is a trace element whose redox chemistry makes it an ideal candidate to trace a range of geochemical processes. Here, we report the first rhenium isotopic measurements ( $\delta^{187}\text{Re}$ ) from river-borne materials to assess the influence of chemical weathering on Re isotopes at continental scale. The  $\delta^{187}\text{Re}$  was measured in water, suspended sediments and bedloads from the Mackenzie River and its main Arctic tributaries in Northwestern Canada. We find that the  $\delta^{187}\text{Re}$  (relative to NIST SRM 989) of river waters ranges from  $-0.05\text{‰}$  to  $+0.07\text{‰}$ , which is generally higher than the corresponding river sediment ( $-0.25\text{‰}$  to  $+0.01\text{‰}$ ). We show that the range of  $\delta^{187}\text{Re}$  in river sediments ( $\sim 0.30\text{‰}$ ) is controlled by a combination of source bedrock isotopic variability (provenance) and modern oxidative weathering processes. After correcting for bedrock variability, the  $\delta^{187}\text{Re}$  of solids appear to be positively correlated with the amount of Re depletion related to oxidative weathering. This correlation, and the offset in  $\delta^{187}\text{Re}$  between river water and sediment, can be explained by preferential oxidation of reactive phases with high  $\delta^{187}\text{Re}$  (i.e. rock organic carbon, sulfide minerals), but could also result from fractionation during oxidation or the influence of secondary weathering processes. Overall, we find that both basin-average bedrock  $\delta^{187}\text{Re}$  ( $\sim -0.05\text{‰}$ ) and dissolved  $\delta^{187}\text{Re}$  ( $\sim -0.01\text{‰}$ ) in the Mackenzie River are lower than the  $\delta^{187}\text{Re}$  of Atlantic seawater ( $+0.12\text{‰}$ ). These observations provide impetus for future work to constrain the Re isotope mass balance of seawater, and assess the potential for secular shifts in its  $\delta^{187}\text{Re}$  values over time, which could provide an additional isotopic proxy to trace current and past redox processes at Earth's Surface.

© 2021 The Author(s). Published by Elsevier B.V. This is an open access article under the CC BY license (<http://creativecommons.org/licenses/by/4.0/>).

## 1. Introduction

Oxidative weathering (OW) of sulfide minerals and petrogenic organic carbon ( $\text{OC}_{\text{petro}}$ ) influences the long-term carbon and oxygen cycles that have governed the evolution of Earth's environment over geologic time (Derry, 2014; Torres et al., 2014). Despite the recognition that OW of  $\text{OC}_{\text{petro}}$  is a source of  $\text{CO}_2$  to the atmosphere, there is still only limited constraint on how these fluxes vary in the present-day (Hilton and West, 2020) and how they have changed in the past (Derry, 2014; Lyons et al., 2019; Petsch, 2014). During OW,  $\text{CO}_2$  is released but is difficult to quantify due to other  $\text{CO}_2$  sources from the modern biosphere and/or carbonate minerals (Soulet et al., 2018). Soluble trace elements that are bound to organic matter (or sulfides) in rocks are also released during OW. Rhenium (Re) has promise as a proxy for tracing the OW flux of  $\text{OC}_{\text{petro}}$  because it is a redox sensitive trace element

enriched in black shales (Colodner et al., 1993) and strongly associated with  $\text{OC}_{\text{petro}}$  (Selby et al., 2007). During OW of  $\text{OC}_{\text{petro}}$ , rhenium is lost from the solid phase (Jaffe et al., 2002) and forms the soluble anion  $\text{ReO}_4^-$  which enters the dissolved load of rivers (Colodner et al., 1993; Miller et al., 2011). Hence, Re has been used as a proxy to quantify OW fluxes in present day river catchments (Dalai et al., 2002; Hilton et al., 2014; Horan et al., 2019).

The ratio of rhenium isotopes in river waters,  $^{187}\text{Re}$  (62.6%) and  $^{185}\text{Re}$  (37.4%), has the potential to improve our understanding of redox reactions during chemical weathering in the present-day, while also leaving a record of such processes in the geological archive. Theoretical calculations (Miller et al., 2015) suggest the potential for significant Re isotope fractionation of  $\sim 1\text{‰}$  during both redox and thiolation processes. However, very few measurements of stable Re isotope composition (reported here as  $\delta^{187}\text{Re} = [((^{187}\text{Re}/^{185}\text{Re})_{\text{sample}} / (^{187}\text{Re}/^{185}\text{Re})_{\text{SRM989}} - 1) \times 1000]$ ) have been made, mostly because of analytical limitations and the low Re concentrations of geological samples (Dellinger et al., 2020; Dickson et al., 2020a; Liu et al., 2017; Miller et al., 2015, 2009). The few studies that exist report a larger range of  $\delta^{187}\text{Re}$  values in shales

\* Corresponding author.

E-mail address: [mathieu.dellinger@durham.ac.uk](mailto:mathieu.dellinger@durham.ac.uk) (M. Dellinger).

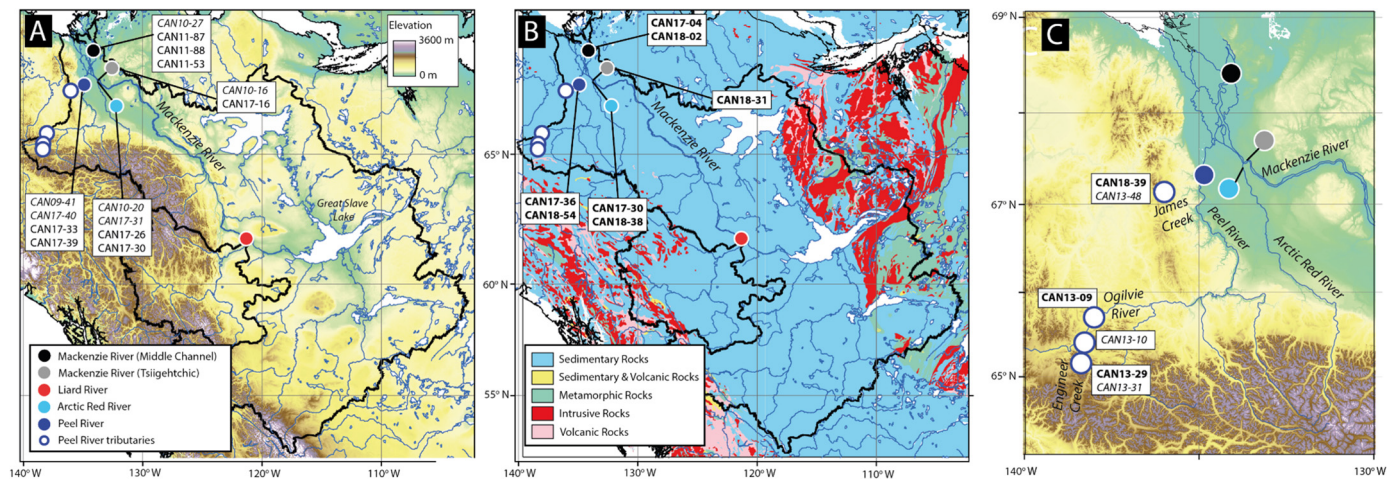


**Fig. 1.** Sample collection in the Mackenzie River basin, adapted from Horan et al. (2019), where circles show the location of samples and individual sample codes are provided (sample code for bedloads is in *italic*, for suspended sediments in plain text, and for dissolved load in **bold**). A) Topography (GDEM 30 Arc Second) showing the main drainage areas (black lines). B) Simplified geological map (Wheeler et al., 1996). C) Detail of topography and sample location in the Mackenzie delta region, the Peel and Arctic Red catchments, and the samples collected from James Creek, the Ogilvie River and Engineer Creek.

( $\sim -0.3$  to  $+0.2\text{‰}$ ) compared to igneous standard reference materials ( $\sim -0.1$  to  $0.0\text{‰}$ ). A study of black shale weathering (Miller et al., 2015) documented a  $\delta^{187}\text{Re}$  decrease of  $\sim 0.3\text{‰}$  in soils compared to unweathered bedrock. This was attributed to either fractionation of Re isotopes during OW, or loss of non-silicate phases with distinct  $\delta^{187}\text{Re}$  leaving behind residual silicate minerals.

Until now, there have been no  $\delta^{187}\text{Re}$  measurements of river water, despite the fact that rivers represent the largest input flux of dissolved Re to the oceans (Miller et al., 2011). Understanding what controls the  $\delta^{187}\text{Re}$  values of river loads could help better constraint modern OW processes, and be crucial for reconstruction of past seawater composition. For instance, the  $\delta^{187}\text{Re}$  of Atlantic seawater appears to be higher ( $\delta^{187}\text{Re} \sim +0.12\text{‰}$ , relative to SRM 989) than mafic igneous rocks (Dickson et al., 2020a), but we do not know the composition of the inputs. Here, for the first time, we investigate the Re isotopic composition of water and sediment carried by the Mackenzie River and its major tributaries. The Mackenzie River basin has been chosen because it has been extensively studied for erosion and weathering (and OW) processes (Carson et al., 1998; Hilton et al., 2015; Millot et al., 2003; Horan et al., 2019) and the behavior of other isotope systems have been explored (e.g., Calmels et al., 2007; Dellinger et al., 2014; Larkin et al., 2021). Here, we find that the  $\delta^{187}\text{Re}$  of water is generally higher than the  $\delta^{187}\text{Re}$  of sediments in each studied river catchment. We discuss the various possible mechanisms that could explain this isotopic difference and explore the implications of these findings for the reconstruction of past OW and ocean redox conditions using Re isotopes.

## 2. The Mackenzie River basin

The Mackenzie river basin (Fig. 1), Canada, is one of the largest rivers on Earth with a total basin area of  $1.78 \times 10^6 \text{ km}^2$ , a mean annual discharge of  $9700 \text{ m}^3 \text{ s}^{-1}$  and a sediment flux of  $130 \text{ Mtyr}^{-1}$  (Carson et al., 1998), making it the largest source of sediment to the Arctic Ocean (Holmes et al., 2002). The Mackenzie River has cold sub-Arctic to Arctic climate with a mean annual temperature  $\sim -4^\circ\text{C}$  and extensive permafrost cover (Millot et al., 2003). The highest discharge and sediment flux occurs at the end of the spring and early summer when the river ice breaks up (Holmes et al., 2002). The Mackenzie River basin can be divided into three main geological units (Millot et al., 2003). In the west, the relief is high and outcropping rocks are dominated by sedimentary rocks (shales, limestones) of the Canadian Cordillera, with

some intruded granitic rocks. The central part of the basin is composed of sedimentary rocks (mostly shales) and glacial deposits. The eastern part of the basin is composed of weakly weathered, metamorphic rocks of the Canadian Shield, whose contribution to the suspended sediment load is negligible (Millot et al., 2003). Most sedimentary rocks are of Palaeozoic age, particularly from the late Devonian (Garzione et al., 1997), and were deposited under various redox conditions (Kabanov, 2019; Ross and Bustin, 2009). The main tributaries are the Liard River draining the Canadian Rockies and the Peel and Arctic Red draining the Mackenzie and Richardson mountains in the northern part of the basin. The average  $\text{OC}_{\text{petro}}$  in bedrocks across the catchment have been previously estimated to be between 0.1% to 0.3% in the Mackenzie River mainstream, but higher ( $\sim 0.6\%$ ) in the Peel catchment (Hilton et al., 2015).

## 3. Sample collection and analytical methods

### 3.1. Sample collection and processing

Samples analyzed in this study (Fig. 1) were collected from field campaigns focused on sampling near the peak water discharge in May–June (in 2011, 2017 and 2018), in July (2009, 2013) and during the falling stage in September (2010). For the Mackenzie main stem, the sampling locations include the Environment Canada gauging stations at Tsiigehtchic and at the Delta Middle channel near Inuvik (Fig. 1). The Peel and Arctic Red rivers, which are the major tributaries that join close to the delta, were sampled at Fort McPherson and Tsiigehtchic respectively. We also sampled some smaller tributaries of the western part of the Peel River basin in 2013 and 2018 (Ogilvie, Upper Engineer Creek and James Creek rivers) that are partly underlain by Devonian  $\text{OC}_{\text{petro}}$ -rich black shales (Kwong et al., 2009).

The sample collection methods were the same for each trip. Suspended sediment depth-profiles and bedloads were collected to characterize the whole range of erosion products carried by large rivers (see details in Dellinger et al., 2014; Hilton et al., 2015; Horan et al., 2019). Briefly, a 5 to 7 L sampler was used to collect water and sediment at a discrete depth in the channel and the sample was then transferred into a sterilized and sealable polyethylene bags. Samples were filtered within 24 h through  $0.2 \mu\text{m}$  polyether-sulfone (PES) filters using pre-cleaned filter units and stored in acid cleaned LDPE bottles. Suspended sediments were immediately

rinsed from the filters using filtered river water into clean amber-glass vials.

For the majority of river water samples for Re isotopic analyses (collected in 2017 and 2018), we use a recently developed method of Dellinger et al. (2020) to pre-concentrate the dissolved Re from river water shortly after filtration in the field. In summary, a known volume of filtered river water of between 1 and 10 L was collected in a new sterile polythene bag and then passed through a BioRad Econo-Pac® 20 mL column containing 2–4 mL of resin AG1-X8 (Dellinger et al., 2020). For rivers which had high dissolved Re concentrations, we were also able to make measurements on previously filtered samples (0.3 to 1 L) which had been stored at 4 °C in the dark.

Overall, we measured the  $\delta^{187}\text{Re}$  of 10 river water samples from 7 different rivers. For the sediment samples, we measured 9 bedload samples for the same rivers for which we measured the dissolved  $\delta^{187}\text{Re}$ , and 9 suspended sediments for the main rivers (Arctic Red, Peel, Mackenzie) attempting to capture surface and deep suspended sediments that have contrasts in their grain size and geochemical composition (Dellinger et al., 2014).

### 3.2. Rhenium concentration measurements

For solid samples, the method for measuring Re concentrations has been described in detail by Dellinger et al. (2020) and is summarized here. All acids were sub-boiling Teflon distilled. A known mass (~0.5 g) of sediment was digested (3 mL 29M HF + 3 mL 16M  $\text{HNO}_3$ ) for 24 to 48 h, followed by one to several steps of aqua regia and 16M  $\text{HNO}_3$  reflux at 150 °C to digest rock organic matter. Care was taken to ensure complete dissolution. The final digestion step was dried down and residue re-dissolved in 20–40 mL of 1 M HCl. Samples were then processed through a column (1 mL of AG1-X8 resin) to isolate Re from the sample matrix, with Re collected with 12.5 mL of 4 M  $\text{HNO}_3$  (Dellinger et al., 2020). The Re fraction was evaporated and re-dissolved in 5 mL 0.5 M  $\text{HNO}_3$ . A 0.1 mL aliquot was taken (the remaining solution was retained for Re isotope measurement) and diluted up to 0.4 mL, including 0.2 mL of 200 ppb tungsten solution as an internal standard. The Re concentration was measured by multicollector inductively coupled plasma mass spectrometry (MC-ICP-MS – Thermo Fisher Scientific Neptune) using calibrating standards and correcting for matrix suppression and instrumental drift using tungsten (W). The standard reference materials measured were reported in Dellinger et al. (2020) and agree well with previous studies. For a few samples, we measured the Re concentration on separate 0.5 g aliquots (between 2 and 9 separate aliquots). The standard deviation on this replicates measurement is better than 8% (1sd). In addition, the Re concentration of some of the samples was also measured by isotope dilution method by Horan et al. (2019), with good agreement between the two methods (see Table S3).

### 3.3. Rhenium isotopic measurements

Re isotopes were measured at the Arthur Holmes Isotope Geology Laboratory, Durham, following the methods described in detail by Dellinger et al. (2020). In summary, a solid mass of 0.5 to 5 g, depending upon the Re concentration, was necessary for accurate Re isotopic measurements (Dellinger et al., 2020). Solid samples were digested and processed through columns as for Re concentration measurements (Section 3.2). However, contrary to Re concentrations, for measuring Re isotopes, this column procedure was repeated two more times (three column passes in total) to ensure removal of residual matrix. Between each column pass, the Re elution fraction was evaporated and treated for 24 h with

concentrated  $\text{HNO}_3$  at 130 °C to destroy any residual organic matter. The Re yield of the column procedure was always greater than 80%. Previous method development revealed no measureable fractionation of Re isotopes for column yields >75% (Dellinger et al., 2020).

The Re in dissolved load samples collected in 2017 and 2018 was pre-concentrated on resin in econopack columns immediately after filtration while in the field. On return to Durham 50 mL of 1 M HCl was passed through the resin to remove some matrix, and Re was eluted with 30 to 40 mL of 8 M  $\text{HNO}_3$  (Dellinger et al., 2020). The eluted Re fraction was further purified through three column passes (see details in Dellinger et al., 2020). Duplicate measurements of sediment sample CAN17-39 returned  $\delta^{187}\text{Re}$  values of  $-0.09 \pm 0.06\text{‰}$  and  $-0.16 \pm 0.07\text{‰}$ , and values of  $+0.01 \pm 0.05\text{‰}$  and  $-0.04 \pm 0.04\text{‰}$  for sample CAN10-20. Repeat measurements of standard Re solution  $\text{HReO}_4$  processed through 1 to 3 columns yielded  $\delta^{187}\text{Re} = +0.22 \pm 0.05\text{‰}$  (2sd,  $n = 16$ ; 5 ng of Re for each analysis) identical non-processed standard solution (Dellinger et al., 2020). Several standard reference materials were repeatedly measured in Dellinger et al. (2020) and during the current study (Table S4), including USGS basalt BCR-2 ( $\delta^{187}\text{Re} = -0.01 \pm 0.03\text{‰}$ , 2sd,  $n = 5$ ; [Re] = 12 ppb), USGS marine mud MAG-1 ( $\delta^{187}\text{Re} = -0.02 \pm 0.08\text{‰}$ , 2sd,  $n = 4$ ; [Re] = 3.7 ppb) and Atlantic seawater OSIL ( $\delta^{187}\text{Re} = +0.10 \pm 0.04\text{‰}$ , 2sd,  $n = 4$ ; [Re] = 7.5 ppt).

### 3.4. Sequential extractions

We conducted a 6-step sequential extraction on three bedload samples (CAN10-16, CAN10-20 and CAN13-31) to investigate the Re content and  $\delta^{187}\text{Re}$  of solid phases that contribute to the bulk sample. A mass of 0.5 g of finely crushed sediment was leached sequentially with: 1) 10 mL of distilled water for 2–3 hours. This water-soluble fraction probably contains free ions and ions complexed with soluble organic matter. It might also contain residual salts from the drying process of the sediments; 2) 5 mL of ammonium acetate 1 M for 2 hours in order to remove exchangeable ions. Note that it may also partly dissolve carbonates; 3) 10 mL 0.05 N HCl for leaching residual exchangeable ions and to partly dissolve carbonates (especially calcite); 4) 10 mL 1 M HCl for 2–3 hours to dissolve remaining carbonates (dolomites, siderite) and potentially some non-pyritic sulfides and iron oxides; 5) strong acid leach (16 M  $\text{HNO}_3$  followed by Aqua regia) at 130–150 °C for 48 h to oxidize  $\text{OC}_{\text{petro}}$  and sulfides. This may also partly leach/dissolve some silicate minerals; 6) 29 M HF–16 M  $\text{HNO}_3$  digestion for dissolving residual silicate minerals. Following each step, samples were centrifuged for 10 minutes and the supernatant was removed. Samples were diluted and measured for Re and other trace element concentrations by quadrupole ICP-MS (See results in Table S2).

## 4. Results

### 4.1. Re isotopes in water and bulk sediments

The  $\delta^{187}\text{Re}$  Re values of river water in the Mackenzie basin ( $n = 10$  samples) span  $0.12\text{‰}$  (Table 1, Fig. 2), ranging from  $-0.05 \pm 0.04\text{‰}$  (Upper Engineer creek) to  $+0.07 \pm 0.03\text{‰}$  (Arctic Red River). For the Mackenzie mainstream, Peel and Arctic Red tributaries, the  $\delta^{187}\text{Re}$  Re value was measured in two different years (2017 and 2018). The difference between the two years (Fig. 2) is  $0.11\text{‰}$  for the Arctic Red River, and within analytical uncertainty for the Peel River ( $0.04\text{‰}$ ) and for the Mackenzie in the Middle channel ( $0.03\text{‰}$ ). The  $\delta^{187}\text{Re}$  Re of suspended sediments ( $n = 8$ ) is lower than the dissolved load, ranging from  $-0.20 \pm 0.07\text{‰}$  (Peel River, 8 m deep) to  $-0.04 \pm 0.05\text{‰}$  (Arctic Red River). The  $\delta^{187}\text{Re}$  Re value of

**Table 1**  
Element concentration and  $\delta^{187}\text{Re}$  data from the Mackenzie dissolved, suspended (SPM) and bedload

Sample name	Collection Date	River	Location	Latitude	Longitude	Depth (m)	Type	$\delta^{187}\text{Re}_{\text{SRM989}}$ (‰)	$\delta^{187}\text{Re}_{\text{NIST3141}}$ (‰)	Overall uncert. on $\delta^{187}\text{Re}$ (‰; 2 SD)	Re (ppt)	Al (ppm)	Na (ppm)	S (ppm)
<i>Bedloads</i>														
CAN10-20	9/7/2010	Red Arctic	Tsiigehtchic	67.43948	−133.75296		Bedload	0.01	−0.27	0.05	4161	47146	3539	1800
CAN10-20 duplicate								−0.04	−0.32	0.04				
CAN17-31	6/5/2017	Red Arctic	Tsiigehtchic	67.43076	−133.78197		Bedload	0.01	−0.27	0.04	5593	53264	3769	
CAN10-16	9/7/2010	Mackenzie	Tsiigehtchic	67.45302	−133.74054		Bedload	−0.24	−0.52	0.05	794	27913	6766	200
CAN10-27	9/8/2010	Mackenzie	Middle Channel	68.44568	−134.21349		Bedload	−0.15	−0.43	0.06	1522	32290	4740	700
CAN09-41	7/21/2009	Peel	Fort McPherson	67.33189	−134.86912		Bedload	−0.08	−0.36	0.04	4021	40620	2708	1265
CAN17-40	6/7/2017	Peel	Fort McPherson	67.32826	−134.86761		Bedload	−0.19	−0.47	0.04	4537	33361	2797	894
CAN13-10	7/20/2013	Ogilvie River	Along Dempster	65.56789	−138.17824		Bedload	−0.10	−0.38	0.04	9453	33075	2463	1509
CAN13-31	7/22/2013	Upper Engineer Creek	Dempster	65.17129	−138.36353		Bedload	−0.24	−0.52	0.04	10881	32816	1996	1055
CAN13-48	7/23/2013	James Creek	Dempster	67.13862	−136.00302		Bedload	−0.18	−0.46	0.04	2838	77544	3420	624
<i>Suspended Particulate Matter (SPM)</i>														
CAN17-26	6/5/2017	Red Arctic	Tsiigehtchic	67.42979	−133.77841	4	SPM	−0.04	−0.32	0.06	7175	68902	3331	3128
CAN17-30	6/5/2017	Red Arctic	Tsiigehtchic	67.42986	−133.77878	0	SPM	−0.04	−0.32	0.05	7665	76485	3272	3220
CAN17-16	6/5/2017	Mackenzie	Tsiigehtchic	67.45313	−133.73657	0	SPM	−0.13	−0.41	0.08	3098	73167	3650	2013
CAN11-87	6/13/2011	Mackenzie	Middle Channel			20	SPM	−0.12	−0.40	0.05	3039	43895	4440	1078
CAN11-88	6/13/2011	Mackenzie	Middle Channel			15	SPM	−0.16	−0.44	0.06	1869	42214	4662	810
CAN17-53	6/10/2017	Mackenzie	Middle Channel	68.41538	−134.11734	0	SPM	−0.14	−0.42	0.08	3112	77104	3806	1765
CAN17-33	6/7/2017	Peel	Fort McPherson	67.32890	−134.86618	7	SPM	−0.20	−0.48	0.07	4563	47183	3287	1905
CAN17-39	6/7/2017	Peel	Fort McPherson	67.32815	−134.86639	0	SPM	−0.09	−0.37	0.06	4514	68521	3850	2238
CAN17-39 duplicate								−0.16	−0.44	0.07				
<i>Dissolved load</i>														
CAN17-30	6/5/2017	Arctic Red	Tsiigehtchic	67.42986	−133.77878		Dissolved	−0.04	−0.32	0.07	2.19		3.7	22.1
CAN18-38	6/9/2018	Arctic Red	Tsiigehtchic	67.42645	−133.77895		Dissolved	0.07	−0.21	0.03	3.19		3.8	38.2
CAN18-31	6/9/2018	Mackenzie	Tsiigehtchic	67.45624	−133.72339		Dissolved	0.00	−0.28	0.03	2.98		6.7	12.4
CAN17-04	6/3/2017	Mackenzie	Middle Channel	68.41781	−134.11600		Dissolved	−0.03	−0.31	0.04	3.12		6.9	13.1
CAN18-02	6/6/2018	Mackenzie	Middle Channel	68.41781	−134.11160		Dissolved	0.00	−0.28	0.03	3.14		6.5	13.1
CAN17-36	6/7/2017	Peel	Fort MacPherson	67.32868	−134.86607		Dissolved	0.03	−0.25	0.05	3.15		4.0	26.1
CAN18-54	6/12/2018	Peel	Fort MacPherson	67.32598	−134.86403		Dissolved	0.07	−0.21	0.03	3.36		4.1	28.4
CAN13-09	7/20/2013	Ogilvie River	First Dempster sight	65.71532	−137.99249		Dissolved	−0.02	−0.31	0.06	6.51		11.3	33.7
CAN13-29	7/22/2013	Upper Engineer Creek	Dempster	65.10129	−138.35582		Dissolved	−0.05	−0.33	0.04	18.68		2.8	60.2
CAN18-39	6/11/2018	James Creek	Dempster Highway	67.13897	−135.99503		Dissolved	0.03	−0.25	0.05	0.25		21.0	132.7



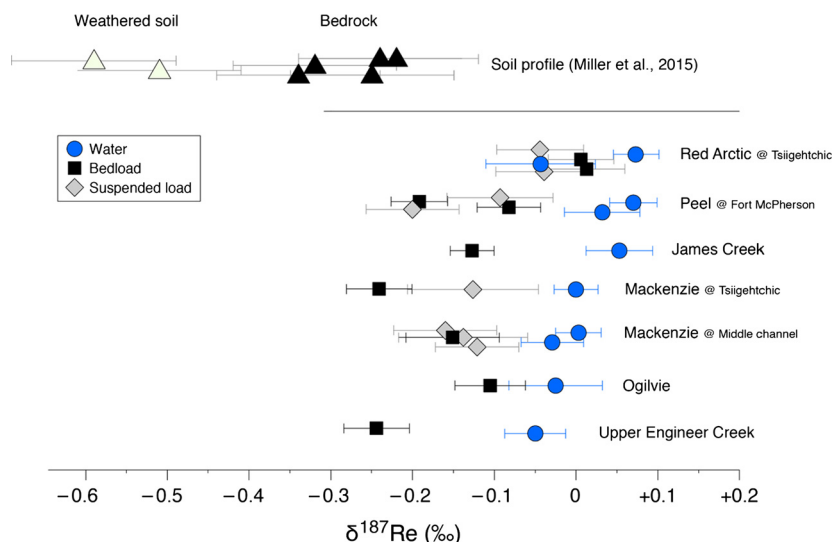


**Fig. 2.** The rhenium isotopic composition ( $\delta^{187}\text{Re}$  relative to SMR989) of river water (blue circles), suspended load (grey diamond) and bedload (black square) from the Mackenzie River basin, for each tributary. For comparison, published measurements from the New Albany black shale weathering profile are shown (Miller et al., 2015). (For interpretation of the colors in the figure(s), the reader is referred to the web version of this article.)

bedloads ( $n = 9$ ) spans  $0.24\text{‰}$ , ranging from  $-0.24 \pm 0.04\text{‰}$  (Upper Engineer Creek) to  $+0.01 \pm 0.04\text{‰}$  (Arctic Red River; Fig. 2). Thus, overall, the bedload and suspended load  $\delta^{187}\text{Re}$  values are broadly similar.

The  $\delta^{187}\text{Re}$  values of the dissolved load are higher than the solid load for each river, with the exception of one water sample from the Arctic Red River (Fig. 2). The  $\delta^{187}\text{Re}$  difference between the dissolved and solid load is minimal for the Arctic Red, but more than  $0.20\text{‰}$  for the Upper Engineer Creek. When compared to published data (Fig. 3), the average  $\delta^{187}\text{Re}$  of Mackenzie River waters is lower than the  $\delta^{187}\text{Re}$  of Atlantic seawater (Dellinger et al., 2020; Dickson et al., 2020a), although there is partial overlap of  $\delta^{187}\text{Re}$  values at the heavier end of the Mackenzie River range (Fig. 3). The  $\delta^{187}\text{Re}$  of Mackenzie river sediments ( $-0.24\text{‰}$  to  $+0.01\text{‰}$ ) is within the range of unweathered rock and higher than the weathered New Albany shale (Miller et al., 2015).

#### 4.2. Sequential extractions

The highest proportion of Re was measured in the organic-sulfide fraction of the extraction, where between 62% and 69% of total Re resided (Table S2). This confirms a strong association between Re and reduced phases ( $\text{OC}_{\text{petro}}$  and sulfides). The Re concentration of the water-soluble fraction was between 9% and 15% of total Re. Most other elements have negligible fractions ( $<5\%$ ) in the water-soluble fraction except for Sulfur (8–10%). A similar water-soluble Re proportion has been reported for initial leaching ( $<3$  hours) of shale rocks (Scheingross et al., 2019). This could relate to leaching of Re complexed with the soluble organic matter, exchangeable Re, or Re from previously oxidized layer in the sediments. A low proportion of Re was measured in the exchangeable fraction ( $<6\%$ ), calcite fraction ( $<6\%$ ) and dolomite-oxides fraction (5% to 9%). In the silicate fraction, the amount of Re relative to the total sample Re was low (3% to 7%), the lowest of any measured chemical element (see range of measured elements in the Table S2). We note that the proportion of Al in the organics-sulfides fraction is between 27% and 37%, which implies some silicates may have been leached or dissolved during this step. The Re/Al mass ratio of the silicate fraction is between  $0.003$  and  $0.004 \times 10^{-6}$ . The difference in concentration between the bulk and the sum of all sequential extraction fractions is less than 5%.

The measured  $\delta^{187}\text{Re}$  for water-soluble, organic-sulfide and silicate fractions are presented in Table S2. The  $\delta^{187}\text{Re}$  of the water-soluble fraction is slightly lower than the bulk  $\delta^{187}\text{Re}$  by  $0.03$  to  $0.11\text{‰}$ . The  $\delta^{187}\text{Re}$  of the organic-sulfide is similar to the bulk for the Mackenzie bedload, but lower by  $0.08\text{‰}$  for the Arctic Red bedload. Finally, the  $\delta^{187}\text{Re}$  of the silicate fraction is much lower than that of the bulk, with  $\delta^{187}\text{Re}$  values of  $-0.22 \pm 0.20\text{‰}$  for the Arctic Red bedload and  $-0.65 \pm 0.26\text{‰}$  for the Mackenzie bedload. These measurements have large uncertainty due to the very low Re content in the silicates.

#### 4.3. Partitioning of Re during chemical weathering

To characterize the behavior of Re during weathering processes, we use the dissolved and suspended Re concentration ( $[\text{Re}]_{\text{diss}}$  and  $[\text{Re}]_{\text{sed}}$ ) and the annual average suspended particulate matter concentration ( $[\text{SPM}]$  in  $\text{g L}^{-1}$ ) to calculate the proportion of Re transported in the dissolved load (noted  $w^{\text{Re}}$ , in %) relative to the total rhenium flux (dissolved + suspended sediments; Supplementary Materials). Rhenium is dominantly transported by the dissolved load in the Mackenzie River ( $w^{\text{Re}} = 77 \pm 3\%$ ), while being equally partitioned between the dissolved and solid load in the Peel ( $w^{\text{Re}} = 47 \pm 7\%$ ) and mostly transported in the solid load in the Arctic Red ( $w^{\text{Re}} = 25 \pm 6\%$ ). Rhenium appears to be more soluble than the majority of other elements in the Mackenzie River, with the exception of sulfur and carbonate-bearing elements (Ca, Mg and Sr), confirming that Re is strongly influenced by chemical weathering processes.

### 5. Discussion

The first measurements of the Re isotopic composition of rivers reveal a large range in the  $\delta^{187}\text{Re}$  of river sediments ( $\delta^{187}\text{Re}_{\text{sed}}$ ) and show that composition of dissolved Re ( $\delta^{187}\text{Re}_{\text{diss}}$ ) is almost always higher than the corresponding  $\delta^{187}\text{Re}_{\text{sed}}$  of each river (Fig. 2). In this discussion, we first show that this large  $\delta^{187}\text{Re}$  variability reflects a combination of variations in the bedrock  $\delta^{187}\text{Re}$  composition ( $\delta^{187}\text{Re}_{\text{rock}}$ ) and a shift in isotopic composition during modern weathering processes. We then discuss the implications for the global Re isotope cycle and for whether  $\delta^{187}\text{Re}$  could act as a tracer of oxidative weathering.

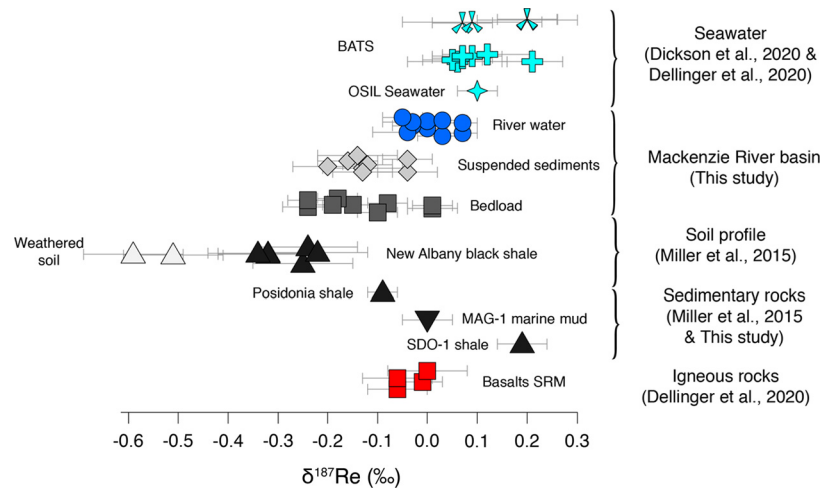


**Fig. 3.** Summary of Re isotopic composition ( $\delta^{187}\text{Re}$ ; all data are normalized to NIST SRM 989) in all published terrestrial materials. Seawater and igneous standard reference materials data are from Dellinger et al. (2020) and Dickson et al. (2020a), the New Albany shale profile from (Miller et al., 2015).

### 5.1. The $\delta^{187}\text{Re}$ and Re composition of bedrocks in the Mackenzie River basin

#### 5.1.1. Variability of bedrock lithological sources of Re and $\delta^{187}\text{Re}$

To understand the controls on  $\delta^{187}\text{Re}$  values and the influence of weathering, we must first determine the extent to which the  $\delta^{187}\text{Re}_{\text{diss}}$  and  $\delta^{187}\text{Re}_{\text{sed}}$  may be controlled by mixture between different bedrocks and/or mineralogical phases with distinct  $\delta^{187}\text{Re}$  and Re concentrations. This has been noted before for Li and Mo isotopes in the Mackenzie River (Dellinger et al., 2014; Horan et al., 2020). Indeed, the large range of reported  $\delta^{187}\text{Re}$  values for shales ( $-0.35\text{‰}$  to  $+0.21\text{‰}$ ; Miller et al., 2015), suggests that lithological variability could be important. While the Mackenzie River basin is dominated by sedimentary rocks, these vary in lithology and depositional age, meaning that they could carry distinct  $\delta^{187}\text{Re}$  values and Re concentrations, depending on the redox state and detrital input of the depositional environment (Dubin and Peucker-Ehrenbrink, 2015; Miller et al., 2015; Sheen et al., 2018).

To assess whether differences in lithology could cause shifts in  $\delta^{187}\text{Re}_{\text{diss}}$  and  $\delta^{187}\text{Re}_{\text{sed}}$ , we first need to characterize the sediment sources (Supplementary Materials). To do this, the element mass ratios V/Al and Cs/Al are used as provenance tracers, where we combine our measurements with additional bedrock values from the Mackenzie basin (Crawford et al., 2019; Kabanov, 2019; Ross and Bustin, 2009). We identify three main rock types with distinct  $\text{OC}_{\text{petro}}$  and Re content: i) “grey shales” mostly from the Paleozoic, with  $\text{OC}_{\text{petro}}/\text{Al}$  mass ratio of 0.03–0.3 and Re/Al values of  $0.02\text{--}0.40 \times 10^{-6}$ ; ii) late Devonian organic-rich shales with high  $\text{OC}_{\text{petro}}/\text{Al}$   $\sim 0.9$  and high Re/Al of  $0.4\text{--}3.0 \times 10^{-6}$ , referred hereafter as “black shale”; and iii) granitic-type igneous rocks with no  $\text{OC}_{\text{petro}}$  and low Re/Al ( $<0.012 \times 10^{-6}$ ). We note that the Late Devonian black shale in the Mackenzie river basin is of similar age and depositional setting as the New Albany Shale studied by Miller et al. (2015), and has similar Re content and Re/Al value. To then quantify the contributions of these three lithological sources, we use V/Al and Cs/Al ratios and a mass-balance calculation (see Supplementary Materials). These show that the majority of Mackenzie River sediments ( $n = 10$  samples) are derived from the grey shales, with a small proportion of igneous rock ( $<30\%$ ) and negligible contribution from black shales ( $<5\%$ ). Exceptions are two bedloads from the Mackenzie main channel, with  $>50\%$  contribution from igneous rocks, and four sediment samples from the Peel, Ogilvie and Upper Engineer Creek with 8–65% contribution from black shales (Table S7). This assessment also highlights that coarse and fine materials can be sourced from different rocks in large rivers.

In terms of the  $\delta^{187}\text{Re}$  values of these lithological sources, we explore this using the  $(\text{Re}/\text{Al})_{\text{sed}}$  ratios (Fig. 4). River sediments sourced partly from the erosion of black shales (Upper Engineer creek and Ogilvie River) have higher  $(\text{Re}/\text{Al})_{\text{sed}}$  ratios and lower  $\delta^{187}\text{Re}$  (Fig. 4), which are most similar to the unweathered New Albany black shale (Miller et al., 2015). In contrast, river sediments mainly sourced from the erosion of grey shales, which dominate in the basin overall, have higher  $\delta^{187}\text{Re}$  and lower Re/Al. Based on these observations (Fig. 4b), we consider the grey shale to have a  $\delta^{187}\text{Re}$  value of  $\sim -0.05\text{‰}$  which is higher than the  $\delta^{187}\text{Re}$  of black shales ( $\delta^{187}\text{Re} \sim -0.30\text{‰}$ ). The value for grey shales should also be considered a minimum value if weathering leads to a decrease of  $\delta^{187}\text{Re}$  as discussed in Section 5.2. To assess the  $\delta^{187}\text{Re}$  of the igneous rock input, we use the composition of the silicate fraction of the sequential extraction. The Re/Al ratio of the silicate fraction of the sequential extraction of Mackenzie River bedloads is  $\sim 0.004 \times 10^{-6}$ , with a  $\delta^{187}\text{Re}$  of  $-0.65 \pm 0.25\text{‰}$  and  $-0.22 \pm 0.20\text{‰}$ , suggesting a low  $\delta^{187}\text{Re}$  and Re/Al of silicates. This Re/Al value is similar to the values inferred for the Upper Continental Crust (Dubin and Peucker-Ehrenbrink, 2015).

#### 5.1.2. Average composition of the unweathered bedrock

It is possible to estimate the average composition of the unweathered bedrock ( $\overline{\delta^{187}\text{Re}}_{\text{rock}}$  and  $\overline{[\text{Re}]}_{\text{rock}}$ ; the hyphen above the parameters indicate “average” unweathered bedrock) in the Mackenzie, Peel and Arctic Red river basins using the calculated  $w^{\text{Re}}$  values and a steady-state mass-balance assessment of dissolved and solid samples (Bouchez et al., 2013). This assumes that the measured present-day suspended sediment flux is similar to the long-term erosion rate (over  $10^3\text{--}10^4$  yr timescale). In the Peel River, the  $^{10}\text{Be}$ -based denudation rate that integrates over  $10^3$  timescales (Wittmann et al., 2020) is the same as present-day suspended sediment flux (Carson et al., 1998). For the Mackenzie main channel, the  $^{10}\text{Be}$ -based erosion rate is slightly higher (by a factor  $\sim 1.5$ ) compared to the present-day sediment flux (Wittmann et al., 2020), possibly due to the paraglacial Mackenzie region landscape still responding to the last glaciation (Church and Slaymaker, 1989). Nevertheless, we assume that denudation in the Mackenzie River is operating at steady-state, and use the steady-state mass-balance approach (Supplementary Materials). We calculate a  $\overline{\delta^{187}\text{Re}}_{\text{rock}}$  value that is similar between the three rivers (Table S5) of between  $-0.06\text{‰}$  and  $-0.03\text{‰}$ , and a  $\overline{(\text{Re}/\text{Al})}_{\text{rock}}$  value between  $0.12 \times 10^{-6}$  and  $0.18 \times 10^{-6}$ . These values are in the range of the estimated composition of the grey shales, the main rock source, as discussed above. These  $\overline{\delta^{187}\text{Re}}_{\text{rock}}$ ,  $\overline{[\text{Re}]}_{\text{rock}}$  and

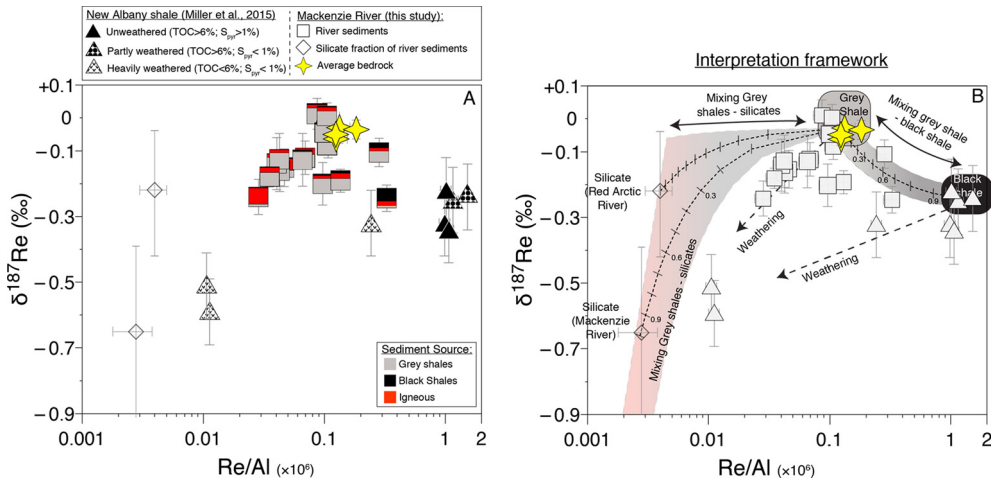


**Fig. 4.** A) The  $\delta^{187}\text{Re}$  (normalized to SRM 989) as a function of the  $\text{Re}/\text{Al}$  (mass ratio) in Mackenzie River sediments (squares, this study) and soil profile samples from the New Albany Shales (triangles, Miller et al., 2015). The composition of the silicate fraction of the sequential extraction for the Arctic Red and Mackenzie bedload is also shown (diamonds). The yellow star is the average bedrock composition of the Mackenzie, Peel and Arctic Red basins calculated by steady-state mass-balance (see section 5.1.2) and the fill corresponds to the lithological proportions (in %wt of Al) for each sediment samples (Supplementary Materials). For the New Albany shales, samples with >6% TOC are considered bedrock (even though some have lost sulfide). B) Data (from part A) are interpreted in a framework of mixing between grey shales and silicates (graduated shading between red and grey), and mixing trend between grey shale and black shales.

$(\text{Re}/\text{Al})_{\text{rock}}$  values allow us to explore the influence of weathering processes on the Re isotopic composition of the river loads (see section 5.3).

## 5.2. Influence of weathering processes on the $\delta^{187}\text{Re}$ of river water and sediments

Having accounted for lithological variability, we find that the  $\delta^{187}\text{Re}_{\text{sed}}$  values derived from the same shale lithology (grey shale) are positively correlated with the  $\text{Re}/\text{Al}$  ratio (Fig. 4). The most Re-depleted samples have the lowest  $\delta^{187}\text{Re}$ . The same trend is observed in the New Albany black shale weathering profile. To explain these patterns and the higher  $\delta^{187}\text{Re}_{\text{diss}}$  values compared to  $\delta^{187}\text{Re}_{\text{sed}}$ , we explore three possible mechanisms (Fig. 5): 1) fractionation of Re isotopes during oxidative weathering, with preferential release of  $^{187}\text{Re}$  into the water (section 5.2.1); 2) secondary removal of dissolved Re in iron oxides or clays with preferential incorporation of  $^{185}\text{Re}$  (section 5.2.2); 3) preferential oxidation of mobile phase(s) with high  $\delta^{187}\text{Re}$  values (section 5.2.3). We argue that the preferential oxidation of mobile phase(s) with high  $\delta^{187}\text{Re}$  composition is the most likely hypothesis (hypothesis 3), to explain the higher  $^{187}\text{Re}$  values in the dissolved load of the Mackenzie. However, we note that based on the limited available measurements, it is not possible to completely exclude the other hypotheses, as explained below.

### 5.2.1. Isotope fractionation during oxidation

Rhenium isotopes may be fractionated during OW processes. An ab-initio calculation (Miller et al., 2015) suggests a positive isotope fractionation (of up to 1.5‰) during oxidation of  $\text{Re}^{\text{IV}}$  to  $\text{Re}^{\text{VII}}\text{O}_4^-$ , with the latter thought to dominate the dissolved Re pool of rivers (Brookins, 1986; Colodner et al., 1993). Isotopic fractionation during initial dissolution stage is possible if a solid surface layer develops (Bouchez et al., 2013; Brantley et al., 2004; Druhan et al., 2015). Eventually, a steady-state is reached where the isotopic composition of the leachate matches the isotopic composition of the dissolving mineral. In most experimental studies, the leachate is enriched in the light isotope due to kinetic effects (Druhan et al., 2015), but fractionation of isotopes associated with redox reactions, such as oxidative weathering, has also been associated with preferential release of the heavy isotope. For example, the first 1% to 10% of leached Fe and Cu from sulfide oxidation exper-

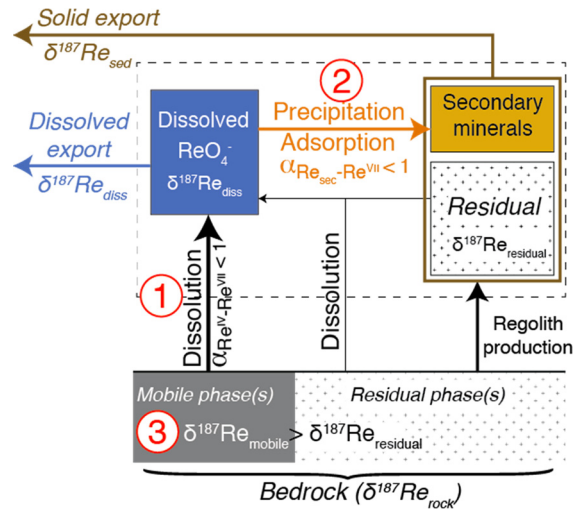


**Fig. 5.** Schematic (inspired from Bouchez et al., 2013) indicating the three possible mechanisms that could explain the higher  $\delta^{187}\text{Re}_{\text{diss}}$  compared to  $\delta^{187}\text{Re}_{\text{sed}}$ : 1) isotopic fractionation during oxidation (fractionation factor between  $\text{Re}^{\text{IV}}$  and  $\text{Re}^{\text{VII}}$ :  $\alpha_{\text{Re}^{\text{IV}}-\text{Re}^{\text{VII}}} = (^{187}\text{Re}/^{185}\text{Re})_{\text{Re}^{\text{IV}}} / (^{187}\text{Re}/^{185}\text{Re})_{\text{Re}^{\text{VII}}} < 1$ ) with preferential release of  $^{187}\text{Re}$  over  $^{185}\text{Re}$  into the dissolved load; 2) isotopic fractionation (fractionation factor between Re in secondary minerals and  $\text{Re}^{\text{VII}}$ :  $\alpha_{\text{Re sec}-\text{Re}^{\text{VII}}} < 1$ ) during Re incorporation into secondary weathering minerals; 3) preferential oxidation of mobile phases with high  $\delta^{187}\text{Re}$  relative to less-mobile phases ("residual") with lower  $\delta^{187}\text{Re}$ . The boxes represent the various Re reservoirs in the weathering zone and bedrock. The arrows represent the Re fluxes.

iments have a heavier isotope composition (Fernandez and Borrok, 2009; Kimball et al., 2009). Isotope fractionation was explained by a change in the oxidation state, combined with the formation of a solid surface layer. A similar process could be considered for Re, i.e. preferential oxidation of  $^{187}\text{Re}$  to the soluble anion  $\text{Re}^{\text{VII}}\text{O}_4^-$ , and formation and leaching of an oxidized layer. This situation could come about due to a high rate of supply of fresh mineral surfaces (i.e. at high erosion rate, and low  $w^{\text{Re}}$ ) and occur where there is cyclic exposure of rocks to OW (Fernandez and Borrok, 2009) and subsequent flushing by fluids that deliver the oxidized products to rivers. The isotopic fractionation can only be expressed if the development of the leached layer is transient, and not at steady-state (Brantley et al., 2004).



The water leach step of the sequential extraction (water-soluble fraction) can provide a constraint on this potential mechanism. Water leaches of Mackenzie River bedload released ~10–15% of the bulk solid Re and have  $\delta^{187}\text{Re}$  values that are equal or slightly lower than the bulk sediment ( $\delta^{187}\text{Re}_{\text{H}_2\text{Oleach}} \leq \delta^{187}\text{Re}_{\text{Sed}}$ ). This suggests that no resolvable fractionation takes place for leaching of >10–15% of rhenium. The fraction of Re in the dissolved load ( $w^{\text{Re}}$ ) in Mackenzie main tributaries is >25% ( $w^{\text{Re}} = 25$  to 78%). This makes it unlikely that  $\delta^{187}\text{Re}_{\text{diss}}$  values would be influenced by this mechanism. Nevertheless, this could still occur upstream in the weathering zone, under the conditions described above (high erosion rate, cyclic exposure of rocks to air oxidation, transient conditions). Dissolution experiments with a lower fraction of rhenium-released (<5–10%) could test this mechanism. Although we cannot completely rule out this mechanism, we conclude that it is unlikely to explain the relative  $^{187}\text{Re}$  enrichment in the Mackenzie river waters.

### 5.2.2. Influence of secondary processes

Dissolved Re may be removed from solution by secondary processes in soils or rivers that include adsorption on clays or Fe-oxides (e.g. Horan et al., 2020 for Mo; Larkin et al., 2021 for Nd) and/or in secondary reduced phases (e.g. secondary sulfides). For this to explain the data, it would be necessary for  $^{185}\text{Re}$  to be preferentially incorporated into secondary products. However, we note that the ion  $\text{ReO}_4^-$  is generally considered stable and soluble under oxic conditions and over an extended pH range (Brookins, 1986; Colodner et al., 1993), although some Re sorption on organic matter (Kim et al., 2004) and clays (Danish et al., 2021) could take place under specific conditions. In the Mackenzie, the relatively high proportion of Re in the dissolved load ( $w^{\text{Re}}$ ) confirms its soluble behavior and so overall, this mechanism seems unlikely.

### 5.2.3. Preferential weathering of high $\delta^{187}\text{Re}$ phase(s)

Preferential weathering of mobile phase(s) (also frequently referred as “reactive” or “labile” in the literature) within rocks may lead to a distinct isotopic composition in waters compared to solids, as shown for several isotopic systems (Bouchez et al., 2013). Indeed, Re is mostly hosted in rock organic matter and sulfides relative to silicates (Jaffe et al., 2002; Miller et al., 2011; Selby et al., 2007), as also shown by our sequential extractions. In the laboratory, the kinetics of sulfide oxidation are faster than those of rock organic matter oxidation (Chang and Berner, 1999), and both are faster than the dissolution of most silicate minerals. Since isotope fractionation during oxidation and/or secondary phase formation are unlikely to be the main fractionating mechanism in the Mackenzie, we suggest that preferential weathering of mobile phase(s) with high  $\delta^{187}\text{Re}$  is the most likely mechanism explaining the enrichment in  $^{187}\text{Re}$  in the dissolved load. Below we explore which mobile and residual phases might represent the best candidates to explain the data in Figs. 2 & 4.

Miller et al. (2015) proposed that preferential weathering of  $\text{OC}_{\text{petro}}$  and sulfides (mobile phases) over silicates (residual phase) could lead to depletion of  $^{187}\text{Re}$  in the rock residues, if silicates have lower  $\delta^{187}\text{Re}$  relative to the non-silicate phases (Fig. 4) (or to put the other way, mobile phases have higher relative  $\delta^{187}\text{Re}$  values). This process would explain why the dissolved load  $\delta^{187}\text{Re}_{\text{diss}}$  values are higher than sediments (Fig. 2). It could also explain why the  $\delta^{187}\text{Re}_{\text{Sed}}$  of sediments are positively correlated to the Re/Al ratio, with a lower Re/Al ratio resulting from a higher proportion of silicate that could reflect partially weathered materials (Fig. 4).

To explore whether a mobile phase (sulfides and/or  $\text{OC}_{\text{petro}}$ ) could have a higher  $\delta^{187}\text{Re}$  than the bulk rock, and that preferential OW of this mobile phase could explain the data, we examine the  $\delta^{187}\text{Re}$  versus the molar Re/S ratio (Fig. 6). The river waters have lower Re/S ratios than the sediments, which is con-

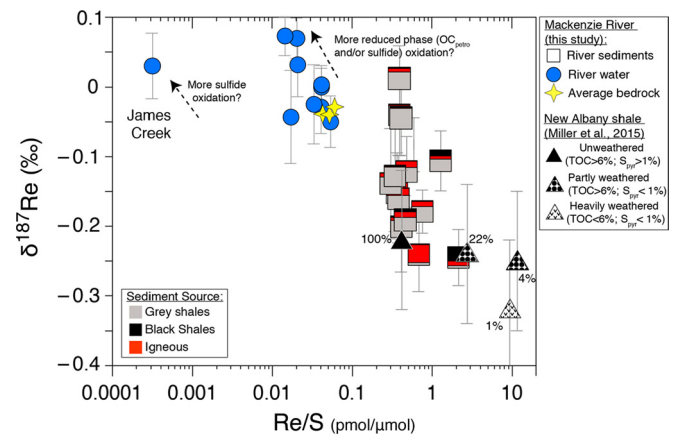


**Fig. 6.** The  $\delta^{187}\text{Re}$  as a function of the molar Re/S ratio of water (circles) and sediment (squares) samples (in pmol/μmol) from the Mackenzie River and the New Albany shale soil profile (triangles, Miller et al., 2015). The percentage number near the New Albany data points corresponds to the proportion of remaining pyrite sulfur from Jaffe et al. (2002).

sistent with preferential weathering of a S-rich phase. Therefore, a simple explanation could be that the higher  $\delta^{187}\text{Re}$  composition of the waters thus reflects the sulfide phase. However, there are two lines of evidence to suggest this is not the case. First, previous work has suggested that dissolved Re in the James Creek River is mostly sourced from sulfides (Horan et al., 2019), based on the high  $\text{SO}_4$  and low Re concentrations (i.e. very low  $\text{Re}/\text{SO}_4 \sim 3 \times 10^{-4}$  pmol/μmol close to the median  $\text{Re}/\text{SO}_4$  of compiled sulfides; Miller et al., 2011). The dissolved  $\delta^{187}\text{Re}$  of James Creek is +0.03‰, slightly lower than the highest dissolved  $\delta^{187}\text{Re}$  of the Arctic Red Rivers (+0.07‰), where more than 85% of the dissolved Re is derived from oxidation of  $\text{OC}_{\text{petro}}$  (Horan et al., 2019). Second, in the New Albany weathering profile (Jaffe et al., 2002; Miller et al., 2015), some samples have near complete loss of sulfides while the  $\text{OC}_{\text{petro}}$  remains (the “partly weathered” samples on Fig. 4 and 6). These show no change in the bulk  $\delta^{187}\text{Re}$  values. This suggests that sulfide oxidation does not influence the  $\delta^{187}\text{Re}$  of the New Albany shale profile. Hence, it appears that the preferential oxidation of sulfides alone cannot explain the higher  $\delta^{187}\text{Re}$  in the dissolved load compared to the sediments.

Alternatively, the high  $\delta^{187}\text{Re}$  phase could be  $\text{OC}_{\text{petro}}$ , or there may be different pools of  $\text{OC}_{\text{petro}}$  with different reactivity that have distinct  $\delta^{187}\text{Re}$  values. It has been shown that Re is associated with a variety of organic compounds, functional groups and bound types in shale organic matter, and is particularly enriched in the high-molecular weight asphaltene fraction of organic matter (Selby et al., 2007). Variability in  $\delta^{187}\text{Re}$  between these different pools could arise from various depositional conditions and/or later-stage thermal maturation (e.g. for Zn isotopes; Dickson et al., 2020b) and metamorphic processes. Selective oxidation of different  $\text{OC}_{\text{petro}}$  pools has been proposed at the soil profile scale (Longbottom and Hockaday, 2019; Petsch, 2014) and at river catchment scale during sediment transport through large river floodplains (e.g. Galy et al., 2008). Indeed, the river water samples reveal a trajectory towards higher  $\delta^{187}\text{Re}$  values while the  $\text{Re}/\text{SO}_4$  ratio remains relatively constant (Fig. 6). This could suggest preferential OW of a reactive  $\text{OC}_{\text{petro}}$  phase with higher  $\delta^{187}\text{Re}$  (mobile phase) relative to less reactive  $\text{OC}_{\text{petro}}$  phases (residual phase). This would also be consistent with the patterns in the solid samples: these do not plot on the mixing zone between the average bedrock and the silicate sequential leaching fraction (Fig. 4B), which would be expected if loss of a mobile phase resulted in only a silicate residue. While we have only two leachate-based estimates of the silicate residue, this discrepancy could be explained if there was an additional host of residual Re in the solids in un-weathered  $\text{OC}_{\text{petro}}$ . We call for



future work to assess the potential role of multiple pools of Re associated with  $\text{OC}_{\text{petro}}$  and its release during oxidative weathering.

### 5.3. Implications for reconstructing oxidative weathering using Re isotopes

Regardless of the mechanisms responsible for Re isotopic fractionation, the observed decrease of  $\delta^{187}\text{Re}$  in solid weathered materials is correlated with the depletion in Re relative to Al for a given rock type (Fig. 4). Taking into account the bedrock variability, we can calculate the isotopic shift related to weathering and the Re-specific mass-transfer coefficient of the solids ( $\tau^{\text{Re}}$ ), using:

$$\Delta^{187}\text{Re}_{\text{sed-rock}} = \delta^{187}\text{Re}_{\text{sed}} - \delta^{187}\text{Re}_{\text{rock}}$$

and

$$\tau^{\text{Re}} = \frac{(\text{Re}/\text{Al})_{\text{sed}}}{(\text{Re}/\text{Al})_{\text{rock}}} - 1$$

To assess the  $(\text{Re}/\text{Al})_{\text{rock}}$  and  $\delta^{187}\text{Re}_{\text{rock}}$  value, it would be preferable to re-calculate the Re/Al and the  $\delta^{187}\text{Re}$  values of each sediment sample to reflect that prior to weathering. However, the large variability in the Re/Al ratio of the grey shale component, likely due to a variable proportion of  $\text{OC}_{\text{petro}}$ , makes this difficult (see supplementary materials). Instead, we use the Mackenzie basin bedrock average  $(\text{Re}/\text{Al})_{\text{rock}}$  and  $\delta^{187}\text{Re}_{\text{rock}}$  values ( $0.13 \times 10^{-6}$  and  $-0.05\text{‰}$ ; the yellow star in Fig. 4) defined by steady-state mass-balance (Section 5.2.2) as a single estimate of the unweathered solid composition for all rivers. Using these values is only justified for Mackenzie River sediments predominantly derived from the grey shale lithology, and for which the contribution of black shales is negligible ( $<5\%$ ). Due to the high Re content in black shale, even a small contribution can significantly shift the average basin-average bedrock  $(\text{Re}/\text{Al})_{\text{rock}}$  toward higher values and the  $\delta^{187}\text{Re}_{\text{rock}}$  toward lower values. Hence, we do not attempt to interpret the Mackenzie river samples with  $>8\%$  black shale contribution in the discussion below because estimating their  $(\text{Re}/\text{Al})_{\text{rock}}$  and  $\delta^{187}\text{Re}_{\text{rock}}$  is not possible.

The  $\Delta^{187}\text{Re}_{\text{sed-rock}}$  is positively correlated with the  $\tau^{\text{Re}}$  ( $r^2 = 0.67$ ; Fig. 7). Both the Mackenzie River sediments and the New Albany shale (Miller et al., 2015) plot on the same trend, which indicates that Re depletion results in a larger isotopic shift ( $\Delta^{187}\text{Re}_{\text{sed-rock}}$ ). Thus, after correcting for  $\delta^{187}\text{Re}$  bedrock differences, the  $\delta^{187}\text{Re}$  values of river sediments and soils can be explained in the same way, i.e. lowering of  $\delta^{187}\text{Re}$  of solids controlled by the proportion of Re depletion during OW. While further work is needed, this indicates that the  $\delta^{187}\text{Re}$  of continental sediments could be used as a proxy for past and present fractional mass loss of  $\text{OC}_{\text{petro}}$  during oxidation.

### 5.4. Implications for the global Re isotopic cycle

We report the first measurements of  $\delta^{187}\text{Re}$  of weathering products in rivers. The supply of Re by rivers is the major source of Re to the ocean, with the sinks being the burial of Re in marine sediments in oxic, suboxic and anoxic settings (Miller et al., 2011; Sheen et al., 2018). The Mackenzie River represents  $\sim 1.1\%$  of the total pre-anthropogenic dissolved Re flux and  $\sim 0.8\%$  of the total present-day flux to the ocean (Miller et al., 2011). The Mackenzie river  $\delta^{187}\text{Re}_{\text{diss}}$  values are lower than Atlantic seawater, with a difference between the  $\delta^{187}\text{Re}$  of the Mackenzie outlet and seawater ( $\Delta^{187}\text{Re}_{\text{input-sw}}$ ) of  $\sim -0.12\text{‰}$ . This confirms the prediction of Dickson et al. (2020a) that the  $\delta^{187}\text{Re}$  of continental input should

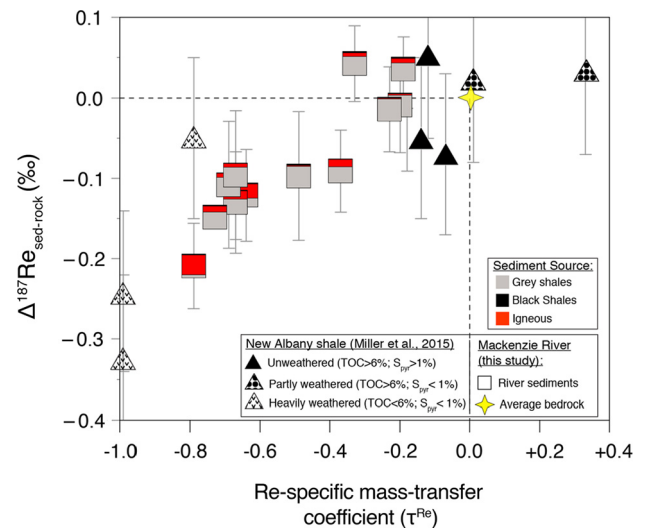


**Fig. 7.** The  $\Delta^{187}\text{Re}_{\text{sed-rock}}$  ratio as the function of the Re-specific mass-transfer coefficient of the solids ( $\tau^{\text{Re}}$ ). Mackenzie sediment samples with  $>8\%$  mass of black shale contribution are not represented (samples CAN17-33, CAN17-40, CAN13-31 and CAN13-10).

be lower than seawater, because Re sinks should favor the incorporation of the  $^{185}\text{Re}$  isotope into marine sediments according to ab-initio calculations (Miller et al., 2015).

To explore these new measurements in the context of the ocean's Re isotopic composition, we revisit the simple Re isotope mass-balance approach of Dickson et al. (2020a). Marine  $\text{ReO}_4^-$  (VII) (residence time of  $1.3 \times 10^5$  yr; Miller et al., 2011) is assumed to be scavenged onto sediments through reduction to  $\text{Re}^{\text{IV}}$ , with a  $\Delta^{187}\text{Re}_{\text{Re(IV)-sw}}$  of up to  $-1.52\text{‰}$ , and/or through thiolation to  $\text{Re}^{\text{VII}}\text{O}_3\text{S}$  (with a  $\Delta^{187}\text{Re}_{\text{Re(VII)O}_3\text{S-sw}}$  of  $-0.33\text{‰}$ ). The  $\Delta^{187}\text{Re}_{\text{input-sw}}$  value ( $-0.12\text{‰}$ ) is lower than both the redox and thiolation fractionation factors: the isotope mass balance cannot be made. There are several possible explanations for this. First, some Re sinks are quantitative (i.e. no fractionation), as it is the case for anoxic or euxinic settings in the modern ocean for other redox sensitive elements (Dickson et al., 2020a). To close the isotopic mass balance, we estimate a minimum proportion of Re removed without fractionation of 8% (if the other sink is reduction to  $\text{Re(IV)}$ ) and a maximum of 33% (with thiolation to  $\text{Re(VII)O}_3\text{S}$ ). Interestingly, this minimum value of 8% for the proportion of quantitative Re removal is close to the proportion of anoxic Re sink in the modern ocean (6–7%) as determined by Sheen et al. (2018). However, there are three other possible explanations which future work needs to assess: 1) there are unaccounted Re sinks (e.g. Danish et al., 2021) with distinct fractionation factor values; 2) the current Re cycle is not at steady-state; and 3) the Mackenzie River is not representative of the average global riverine  $\delta^{187}\text{Re}_{\text{diss}}$ . Our study highlights the importance of assessing whether  $\delta^{187}\text{Re}_{\text{diss}}$  is higher than rocks in other settings, and determining the variability of the  $\delta^{187}\text{Re}_{\text{diss}}$  values of continental inputs. Only with this information can we begin to probe how the Re isotopic composition of seawater could serve as a measure of past changes in ocean redox and/or OW on the continents through Earth's history.

## 6. Conclusions

We present the first measurements of Re isotopic compositions ( $\delta^{187}\text{Re}$ ) in river water and sediments from the Mackenzie River basin (Northwest Canada). The  $\delta^{187}\text{Re}$  values of river water range between  $-0.05$  and  $+0.07\text{‰}$  and from  $-0.27$  to  $+0.01\text{‰}$  in river sediments. The range of  $\delta^{187}\text{Re}$  values in solids (suspended sediments and bedloads) can be explained by a combination of source

variability and the influence of oxidative weathering. The  $\delta^{187}\text{Re}$  of the dissolved Re is generally higher (by up to 0.2‰) than the  $\delta^{187}\text{Re}$  of river sediments. This indicates that oxidative weathering processes lead to an enrichment of  $^{187}\text{Re}$  in the dissolved load (the product of oxidative weathering) and we observe a depletion of  $^{187}\text{Re}$  in river sediments (the residue of oxidative weathering) relative to the source bedrock. This result is consistent with Miller et al. (2015) showing decrease of  $\delta^{187}\text{Re}$  in weathered material from a soil profile.

The possible mechanisms that can explain this isotopic shift include preferential oxidation of high  $\delta^{187}\text{Re}$  phases (e.g.  $\text{OC}_{\text{petro}}$  and/or sulfides) and/or fractionation during oxidation and/or influence of secondary processes. Sequential extraction measurements and mass-balance mixing suggest that preferential weathering of  $\text{OC}_{\text{petro}}$  could explain the data, but fractionation during oxidation or secondary processes could also play a role. Regardless of the mechanisms behind the observed patterns, the difference between the  $\delta^{187}\text{Re}$  of sediments and  $\delta^{187}\text{Re}$  of the bedrock appears to be positively correlated with the Re weathering intensity of sediments. This suggests that  $\delta^{187}\text{Re}$  could be a promising proxy for tracing past and present oxidative weathering processes.

### Declaration of competing interest

The authors declare that they have no known competing financial interests or personal relationships that could have appeared to influence the work reported in this paper.

### Acknowledgements

Fieldwork, method development and initial measurements were funded by a European Research Council Starting Grant ROC- $\text{CO}_2$  to RGH (ERC-StG-2015, project 678779) and subsequent work funded by a Natural Environment Research Council, UK Standard Grant to RGH and MD (NE/T001119/1). We thank Julie Prytulak, Kevin Burton and Alex Dickson for constructive discussions, and Valier Galy, Damien Calmels, Edward Tipper, Hugo Chauvet, Melissa Schwab, Christina Larkin, Edwin Amos, and Jotis Baronas for field assistance. We thank Martin West and Amanda Hayton for additional laboratory support. This manuscript benefited greatly from thoughtful comments from the Associate Editor L. Derry, and two anonymous reviewers.

### Appendix A. Supplementary material

Supplementary material related to this article can be found online at <https://doi.org/10.1016/j.epsl.2021.117131>.

### References

- Bouchez, J., Blanckenburg, F., von Schuessler, J.A., 2013. Modeling novel stable isotope ratios in the weathering zone. *Am. J. Sci.* 313, 267–308. <https://doi.org/10.2475/04.2013.01>.
- Brantley, S.L., Liermann, L.J., Guynn, R.L., Anbar, A., Icopini, G.A., Barling, J., 2004. Fe isotopic fractionation during mineral dissolution with and without bacteria. *Geochim. Cosmochim. Acta* 68, 3189–3204. <https://doi.org/10.1016/j.gca.2004.01.023>.
- Brookins, D.G., 1986. Rhenium as analog for fissionogenic technetium: Eh–pH diagram (25 °C, 1 bar) constraints. *Appl. Geochem.* 1, 513–517. [https://doi.org/10.1016/0883-2927\(86\)90056-9](https://doi.org/10.1016/0883-2927(86)90056-9).
- Calmels, D., Gaillardet, J., Brenot, A., France-Lanord, C., 2007. Sustained sulfide oxidation by physical erosion processes in the Mackenzie River basin: climatic perspectives. *Geology* 35, 1003–1006. <https://doi.org/10.1130/G24132A.1>.
- Carson, M.A., Jasper, J.N., Conly, F.M., 1998. Magnitude and sources of sediment input to the Mackenzie Delta, Northwest territories, 1974–94. *Arctic* 51, 116–124.
- Chadwick, O.A., Brimhall, G.H., Hendricks, D.M., 1990. From a black to a gray box—a mass balance interpretation of pedogenesis. *Geomorphology* 3 (3–4), 369–390.
- Chang, S., Berner, R.A., 1999. Coal weathering and the geochemical carbon cycle. *Geochim. Cosmochim. Acta* 63, 3301–3310. [https://doi.org/10.1016/S0016-7037\(99\)00252-5](https://doi.org/10.1016/S0016-7037(99)00252-5).
- Church, M., Slaymaker, O., 1989. Disequilibrium of Holocene sediment yield in glaciated, British Columbia. *Nature* 337, 452–454. <https://doi.org/10.1038/337452a0>.
- Colodner, D., Sachs, J., Ravizza, G., Turekian, K., Edmond, J., Boyle, E., 1993. The geochemical cycle of rhenium: a reconnaissance. *Earth Planet. Sci. Lett.* 117, 205–221. [https://doi.org/10.1016/0012-821X\(93\)90127-U](https://doi.org/10.1016/0012-821X(93)90127-U).
- Crawford, I., Layton-Matthews, D., Peter, J., Gadd, M., Voinot, A., 2019. Toward the Application of Molybdenum and Thallium Isotopes as Indicators of Paleoredox Conditions and Genesis of Hyper-Enriched Black Shale (HEBS) Deposits. Peel, River, Yukon.
- Dalai, T.K., Singh, S.K., Trivedi, J.R., Krishnaswami, S., 2002. Dissolved rhenium in the Yamuna river system and the Ganga in the Himalaya: role of black shale weathering on the budgets of Re, Os, and U in rivers and  $\text{CO}_2$  in the atmosphere. *Geochim. Cosmochim. Acta* 66, 29–43. [https://doi.org/10.1016/S0016-7037\(01\)00747-5](https://doi.org/10.1016/S0016-7037(01)00747-5).
- Danish, M., Tripathy, G.R., Mitra, S., Rout, R.K., Raskar, S., 2021. Non-conservative removal of dissolved rhenium from a coastal lagoon: clay adsorption versus biological uptake. *Chem. Geol.* 120378.
- Dellinger, M., Gaillardet, J., Bouchez, J., Calmels, D., Galy, V., Hilton, R.G., Louvat, P., France-Lanord, C., 2014. Lithium isotopes in large rivers reveal the cannibalistic nature of modern continental weathering and erosion. *Earth Planet. Sci. Lett.* 401, 359–372. <https://doi.org/10.1016/j.epsl.2014.05.061>.
- Dellinger, M., Hilton, R.G., Nowell, G.M., 2020. Measurements of rhenium isotopic composition in low-abundance samples. *J. Anal. At. Spectrom.* 35, 377–387. <https://doi.org/10.1039/C9JA00288J>.
- Derry, L.A., 2014. 12.9 - Organic carbon cycling and the lithosphere. In: Turekian, H.D.H.K. (Ed.), *Treatise on Geochemistry*, second edition. Elsevier, Oxford, pp. 239–249.
- Dickson, A.J., Hsieh, Y.-T., Bryan, A., 2020a. The rhenium isotope composition of Atlantic Ocean seawater. *Geochim. Cosmochim. Acta*. <https://doi.org/10.1016/j.gca.2020.02.020>.
- Dickson, A.J., Idiz, E., Porcelli, D., van den Boorn, S.H.J.M., 2020b. The influence of thermal maturity on the stable isotope compositions and concentrations of molybdenum, zinc and cadmium in organic-rich marine mudrocks. In: *New Developments in Geochemical Proxies for Paleoclimatographic Research*. *Geochim. Cosmochim. Acta* 287, 205–220. <https://doi.org/10.1016/j.gca.2019.11.001>.
- Druhan, J.L., Brown, S.T., Huber, C., 2015. Isotopic gradients across fluid–mineral boundaries. *Rev. Mineral. Geochem.* 80, 355–391. <https://doi.org/10.2138/rmg.2015.80.11>.
- Dubin, A., Peucker-Ehrenbrink, B., 2015. The importance of organic-rich shales to the geochemical cycles of rhenium and osmium. *Chem. Geol.* 403, 111–120. <https://doi.org/10.1016/j.chemgeo.2015.03.010>.
- Fernandez, A., Borrok, D.M., 2009. Fractionation of Cu, Fe, and Zn isotopes during the oxidative weathering of sulfide-rich rocks. *Chem. Geol.* 264, 1–12. <https://doi.org/10.1016/j.chemgeo.2009.01.024>.
- Galy, V., Beyssac, O., France-Lanord, C., Eglinton, T., 2008. Recycling of graphite during Himalayan erosion: a geological stabilization of carbon in the crust. *Science* 322, 943–945. <https://doi.org/10.1126/science.1161408>.
- Garzione, C.N., Patchett, P.J., Ross, G.M., Nelson, J., 1997. Provenance of Paleozoic sedimentary rocks in the Canadian cordilleran miogeocline: a Nd isotopic study. *Can. J. Earth Sci.* 34, 1603–1618.
- Hilton, R.G., Gaillardet, J., Calmels, D., Birck, J.-L., 2014. Geological respiration of a mountain belt revealed by the trace element rhenium. *Earth Planet. Sci. Lett.* 403, 27–36. <https://doi.org/10.1016/j.epsl.2014.06.021>.
- Hilton, R.G., Galy, V., Gaillardet, J., Dellinger, M., Bryant, C., O'Regan, M., Gröcke, D.R., Coxall, H., Bouchez, J., Calmels, D., 2015. Erosion of organic carbon in the Arctic as a geological carbon dioxide sink. *Nature* 524, 84–87. <https://doi.org/10.1038/nature14653>.
- Hilton, R.G., West, A.J., 2020. Mountains, erosion and the carbon cycle. *Nat. Rev. Earth Environ.* 1, 284–299. <https://doi.org/10.1038/s43017-020-0058-6>.
- Holmes, R.M., McClelland, J.W., Peterson, B.J., Shiklomanov, I.A., Shiklomanov, A.I., Zhulidov, A.V., Gordeev, V.V., Bobrovitskaya, N.N., 2002. A circumpolar perspective on fluvial sediment flux to the Arctic Ocean. *Glob. Biogeochem. Cycles* 16, 1098. <https://doi.org/10.1029/2001GB001849>.
- Horan, K., Hilton, R.G., Dellinger, M., Tipper, E., Galy, V., Calmels, D., Selby, D., Gaillardet, J., Ottley, C.J., Parsons, D.R., Burton, K.W., 2019. Carbon dioxide emissions by rock organic carbon oxidation and the net geochemical carbon budget of the Mackenzie River basin. *Am. J. Sci.* 319, 473–499. <https://doi.org/10.2475/06.2019.02>.
- Horan, K., Hilton, R.G., McCoy-West, A.J., Selby, D., Tipper, E.T., Hawley, S., Burton, K.W., 2020. Unravelling the controls on the molybdenum isotope ratios of river waters. *Geochim. Perspect. Lett.*, 1–6. <https://doi.org/10.7185/geochemlet.2005>.
- Jaffe, L.A., Peucker-Ehrenbrink, B., Petsch, S.T., 2002. Mobility of rhenium, platinum group elements and organic carbon during black shale weathering. *Earth Planet. Sci. Lett.* 198, 339–353. [https://doi.org/10.1016/S0012-821X\(02\)00526-5](https://doi.org/10.1016/S0012-821X(02)00526-5).
- Kabanov, P., 2019. Devonian (c. 388–375 Ma) Horn River group of Mackenzie platform (NW Canada) is an open-shelf succession recording oceanic anoxic events. *J. Geol. Soc.* 176, 29–45. <https://doi.org/10.1144/jgs2018-075>.
- Kim, E., Benedetti, M.F., Boulégué, J., 2004. Removal of dissolved rhenium by sorption onto organic polymers: study of rhenium as an analogue of radioactive

- technetium. *Water Res.* 38, 448–454. <https://doi.org/10.1016/j.watres.2003.09.033>.
- Kimball, B.E., Mathur, R., Dohnalkova, A.C., Wall, A.J., Runkel, R.L., Brantley, S.L., 2009. Copper isotope fractionation in acid mine drainage. *Geochim. Cosmochim. Acta* 73, 1247–1263. <https://doi.org/10.1016/j.gca.2008.11.035>.
- Kwong, Y.T.J., Whitley, G., Roach, P., 2009. Natural acid rock drainage associated with black shale in the Yukon territory, Canada. In: *Natural Low-pH Environments Unaffected by Human Activity*. *Appl. Geochem.* 24, 221–231. <https://doi.org/10.1016/j.apgeochem.2008.11.017>.
- Larkin, C.S., Piotrowski, A.M., Hindshaw, R.S., Bayon, G., Hilton, R.G., Baronas, J.J., Dellinger, M., Wang, R., Tipper, E.T., 2021. Constraints on the source of reactive phases in sediment from a major Arctic river using neodymium isotopes. *Earth Planet. Sci. Lett.* 565, 116933.
- Liu, R., Hu, L., Humayun, M., 2017. Natural variations in the rhenium isotopic composition of meteorites. *Meteorit. Planet. Sci.* 52, 479–492. <https://doi.org/10.1111/maps.12803>.
- Longbottom, T.L., Hockaday, W.C., 2019. Molecular and isotopic composition of modern soils derived from kerogen-rich bedrock and implications for the global C cycle. *Biogeochemistry* 143, 239–255. <https://doi.org/10.1007/s10533-019-00559-4>.
- Lyons, S.L., Baczynski, A.A., Babila, T.L., Bralower, T.J., Hajek, E.A., Kump, L.R., Polites, E.G., Self-Trail, J.M., Trampush, S.M., Vornlocher, J.R., Zachos, J.C., Freeman, K.H., 2019. Palaeocene–Eocene thermal maximum prolonged by fossil carbon oxidation. *Nat. Geosci.* 12, 54–60. <https://doi.org/10.1038/s41561-018-0277-3>.
- Miller, C.A., Peucker-Ehrenbrink, B., Ball, L., 2009. Precise determination of rhenium isotope composition by multi-collector inductively-coupled plasma mass spectrometry. *J. Anal. At. Spectrom.* 24, 1069–1078.
- Miller, C.A., Peucker-Ehrenbrink, B., Schauble, E.A., 2015. Theoretical modeling of rhenium isotope fractionation, natural variations across a black shale weathering profile, and potential as a paleoredox proxy. *Earth Planet. Sci. Lett.* 430, 339–348. <https://doi.org/10.1016/j.epsl.2015.08.008>.
- Miller, C.A., Peucker-Ehrenbrink, B., Walker, B.D., Marcantonio, F., 2011. Re-assessing the surface cycling of molybdenum and rhenium. *Geochim. Cosmochim. Acta* 75, 7146–7179. <https://doi.org/10.1016/j.gca.2011.09.005>.
- Millot, R., Gaillardet, J., Jérôme, Dupré, B., Allègre, C.J., 2003. Northern latitude chemical weathering rates: clues from the Mackenzie River basin, Canada. *Geochim. Cosmochim. Acta* 67, 1305–1329. [https://doi.org/10.1016/S0016-7037\(02\)01207-3](https://doi.org/10.1016/S0016-7037(02)01207-3).
- Petsch, S.T., 2014. 12.8 - weathering of organic carbon. In: Turekian, H.D.H.K. (Ed.), *Treatise on Geochemistry, second edition*. Elsevier, Oxford, pp. 217–238.
- Ross, D.J.K., Bustin, R.M., 2009. Investigating the use of sedimentary geochemical proxies for paleoenvironment interpretation of thermally mature organic-rich strata: examples from the Devonian–Mississippian shales, Western Canadian sedimentary basin. *Chem. Geol.* 260, 1–19. <https://doi.org/10.1016/j.chemgeo.2008.10.027>.
- Scheingross, J.S., Hovius, N., Dellinger, M., Hilton, R.G., Repasch, M., Sachse, D., Gröcke, D.R., Vieth-Hillebrand, A., Turowski, J.M., 2019. Preservation of organic carbon during active fluvial transport and particle abrasion. *Geology* 47, 958–962. <https://doi.org/10.1130/G46442.1>.
- Selby, D., Creaser, R.A., Fowler, M.G., 2007. Re–Os elemental and isotopic systematics in crude oils. *Geochim. Cosmochim. Acta* 71, 378–386. <https://doi.org/10.1016/j.gca.2006.09.005>.
- Sheen, A.L., Kendall, B., Reinhard, C.T., Creaser, R.A., Lyons, T.W., Bekker, A., Poulton, S.W., Anbar, A.D., 2018. A model for the oceanic mass balance of rhenium and implications for the extent of Proterozoic ocean anoxia. *Geochim. Cosmochim. Acta* 227, 75–95. <https://doi.org/10.1016/j.gca.2018.01.036>.
- Soulet, G., Hilton, R.G., Garnett, M.H., Dellinger, M., Croissant, T., Ogrič, M., Klotz, S., 2018. Technical note: in situ measurement of flux and isotopic composition of CO<sub>2</sub> released during oxidative weathering of sedimentary rocks. *Biogeochemistry* 15, 4087–4102. <https://doi.org/10.5194/bg-15-4087-2018>.
- Torres, M.A., West, A.J., Li, G., 2014. Sulphide oxidation and carbonate dissolution as a source of CO<sub>2</sub> over geological timescales. *Nature* 507, 346–349. <https://doi.org/10.1038/nature13030>.
- Wheeler, J.O., Hoffman, P.F., Card, K.D., Davidson, A., Sanford, B.V., Okulitch, A.V., Roest, W.R., 1996. Geological map of Canada: natural resources Canada. "A" Series Map 1860A, 3 sheets, 1:5,000,000. <https://doi.org/10.4095/208175>.
- Wittmann, H., Oelze, M., Gaillardet, J., Garzanti, E., von Blanckenburg, F., 2020. A global rate of denudation from cosmogenic nuclides in the Earth's largest rivers. *Earth-Sci. Rev.* 204, 103147. <https://doi.org/10.1016/j.earscirev.2020.103147>.